Characterization of coral-associated microbial aggregates (CAMAs) within tissues of the coral *Acropora hyacinthus*

Naohisa Wada[1,2,7], Mizuki Ishimochi[2,3], Taeko Matsui[2], F. Joseph Pollock[4,7,8], Sen-Lin Tang[1], Tracy D. Ainsworth[5], Bette L. Willis[6,7], Nobuhiro Mano[2,†], David G. Bourne[6,7,9,†]

[1]Biodiversity Research Center, Academia Sinica, Nangang, Taipei, Taiwan
[2]Department of Marine Science and Resources, College of Bioresource Science, Nihon University, Fujisawa, Kanagawa, Japan
[3]Faculty of Science, University of the Ryukyus, Nishihara, Okinawa 903-0213, Japan
[4]The Nature Conservancy, Caribbean Division, Coral Gables, FL 33134
[5]School of Biological, Earth and Environmental Science, University of New South Wales, Sydney, NSW, Australia
[6]College of Science and Engineering, James Cook University, Townsville, QLD, Australia
[7]AIMS@JCU, Townsville, QLD, Australia
[8]The Pennsylvania State University, State College, PA, USA
[9]Australian Institute of Marine Science, Townsville, QLD, Australia

†Equal correspond authors
Dr. Nobuhiro Mano (mano.nobuhiro@nihon-u.ac.jp) Department of Marine Science and Resources, College of Bioresource Science, Nihon University, Fujisawa, Kanagawa, 252-0813 Japan. Phone +81 466 84 3357
Dr. David G. Bourne (david.bourne@jcu.edu.au) College of Science and Engineering, James Cook University, Townsville, QLD, 4811 Australia. Phone +61 7 47814790

Kew Words: Coral Microbiome, Coral Tissue, Bacterial Aggregates, Fluorescent *in situ* Hybridisation

Abstract

Bacterial diversity associated with corals has been studied extensively, however, localization of bacterial associations within the holobiont is still poorly resolved. Here we provide novel insight into the localization of coral-associated microbial aggregates (CAMAs) within tissues of the coral *Acropora hyacinthus* using histological and fluorescent *in situ* hybridization approaches. In total, 318 CAMAs were characterized and shown to be distributed extensively throughout coral tissues collected from five sites in Japan and Australia. Density of basophilic CAMAs was typically higher at inshore sites (20.13 per cm^2 at inshore sites in Okinawa, Japan; 5.43 per cm^2 at inner shelf sites in the northern Great Barrier Reef) than at offshore sites on the GBR (0 to 1.1 per cm^2). CAMAs were randomly distributed across the six coral tissue regions investigated. Within each CAMA, bacterial cells had similar morphological characteristics, but bacterial morphologies varied among CAMAs, with at least five distinct types identified. Identifying the location of microorganisms associated with the coral host is a prerequisite for understanding their contributions to fitness. Localization of tissue-specific communities housed within CAMAs is particularly important, as these communities are potentially important contributors to vital metabolic functions of the holobiont.

Introduction

Scleractinian corals associate with a broad consortia of microorganisms, including endosymbiont dinoflagellates (*Symbiodiniaceae*), protozoa, fungi, bacteria, archaea and viruses, which collectively are termed the coral holobiont [1–3]. The importance of symbiotic dinoflagellates in provisioning the coral host with essential nutrients through translocated photosynthates has been well established [e.g.,4], however the roles of other microorganisms within the holobiont are less well understood. Some of the functions attributed to coral-associated microbiota include supply of essential nutrients and vitamins through processes such as nitrogen fixation [5–8] and metabolizing dimethylsulfoniopropionate (DMSP) to produce biologically important byproducts like dimethylsulfide [9]. The coral microbiome is also likely important for directly facilitating disease resistance through production of antimicrobials [10,11] or indirectly through microhabitat colonization that excludes opportunistic organism [12,13].

Corals are considered simple metazoans, but despite their basal phylogenetic position, they nevertheless form complex three-dimensional structures. Anatomically, the coral polyp consists of an outer mucus layer, two cell layers containing endosymbiotic dinoflagellates (inner layer) and nematocysts (outer layer), an external calcium carbonate skeleton, and a gastrovascular system that includes the coelenteron and connecting channels [14]. Within all these microhabitat niches, bacteria can reside as either transient communities or established symbionts with putative functional roles that may be positive, neutral or negative to the coral holobiont [15]. A multitude of studies have reported on the diversity of the coral microbiome, in some cases finding conserved

70 microbial communities associated with some coral species, and in others finding
71 shifting microbiomes that reflect varying geographic, temporal or health status patterns
72 [16–20]. To understand the significance of coral microbiome associations, care must be
73 exercised so that diversity patterns reflect the specific ecological niche that these
74 communities inhabit, such as the surface mucus layer, tissue layers, and/or the skeleton
75 [21–28]. Defining the locations of specific microorganisms is essential for elucidating the
76 importance of their role within the holobiont. For example, mucus bacteria are more
77 likely to have a loose association with the coral host, being sloughed off as the mucus is
78 exuded from the corals [29]. Conversely tissue-associated microorganisms are potentially
79 more integrated in shared metabolic pathways and may reside in specific associations
80 with host coral as a consequence of potential host selection [5,20].

81 To date, few studies have precisely localized bacterial communities within
82 coral tissues. Studies that have focused on localization often find that bacterial
83 communities within coral cell layers (i.e. epidermal and gastrodermal layers) form
84 aggregations termed coral-associated microbial aggregates (CAMAs) [30,31]. CAMAs
85 were first reported as potential pathogens when observed within healthy tissues of
86 Caribbean corals displaying signs of white band disease [32,33]. Further studies
87 subsequently reported that CAMAs are widespread in tissues of healthy corals sampled
88 from geographically dispersed areas [31,33,34]. To date, CAMAs have been reported from 5
89 species of corals in the Caribbean [32,33] and 24 species from the Indo-Pacific [31], although
90 their frequency varies among coral genera, with the genera *Acropora*, *Porites*, and
91 *Pocillopora* most commonly hosting bacterial aggregates [31]. Identification of the

92 microorganisms that constitute these CAMAs has been poorly resolved. Neave et al.
93 (2016) visualized aggregates (i.e., "cyst-like aggregations") of *Endozoicomonas* within
94 tissues of *Stylophora pistillata* at the interface of the epidermis and gastrodermis in
95 samples taken from widely-separated biogeographic regions [35]. However, the fine-scale
96 spatial distributions of microorganisms and potential microhabitat-associated structure
97 of the microbiome still have not been clarified. Here, we visualize the localization,
98 distribution and morphology of CAMAs associated with the coral *Acropora hyacinthus*
99 sampled from Sesoko Island, Okinawa, Japan and sites in the northern Great Barrier
100 Reef (GBR) Australia located along an inshore to offshore gradient.
101

102 ## Results

103 *Comparison of CAMA abundance among geographic locations*

104 At the time of field collection, all 48 colonies of *A. hyacinthus* sampled from
105 the 5 geographic locations (see **Fig. 1**) appeared visually healthy. This was confirmed
106 by subsequent histological analyses, which found that all tissues displayed normal cell
107 morphology, including no signs of fragmentation, wound repair or necrosis (as per
108 criteria in Work and Aeby 2011). In total, 318 CAMAs were characterized via histology
109 within coral tissues from the 48 samples. The vast majority stained basophilic (95.9%)
110 using the standard haemotoxylin and eosin stain, compared to only 4.1 % staining
111 eosinophilic (**Fig. 2**). Of the 48 colonies collected across all five sites, CAMAs were
112 detected in 27 of the colonies (~56%). At one site (Sesoko Island), tissues from all 10
113 colonies sampled contained CAMAs (**Fig. 2c**), whereas at the other four sites, CAMAs

were observed only in some of the coral tissues sampled. For example, clear CAMAs were visible in 80% of Inner Shelf samples, 30% of Lizard Island, 25% of Outer Shelf, and 40% of Orpheus Island samples (n=10 samples at all sites, except at the Outer Shelf site where n=8 samples) (**Fig. 2c**). In general, the abundance of CAMAs was significantly higher at the inshore Sesoko Island site than at more offshore sites (Lizard Island, Outer Shelf, and Orpheus Island sites; $p < 0.05$).

The density of basophilic CAMAs in tissues was significantly higher for the Sesoko Island and Inner Shelf sites compared to the other three sites, with 20.13±17.1 and 5.43±8.7 basophilic CAMAs detected per cm^2 of tissue at these two sites, respectively (**Fig. 2d**; $p < 0.05$). In one sample from Sesoko Island, 48.9 CAMAs were detected per cm^2 of tissue, the greatest density of CAMAs observed in the 48 samples investigated. This is in contrast to an average of 0.28±0.4, 0 and 1.1±2.3 CAMAs per cm^2 for the Lizard Island, Outer Shelf and Orpheus Island samples, respectively (**Fig. 2d**). In contrast, the abundance of eosinophilic CAMAs did not differ significantly among the five sites, although the density of CAMAs was higher at the Outer Shelf, GBR site (1.3±3.5 CAMAs per cm^2, **Fig. 2d**) than at other sites (Sesoko Island: 0 CAMAs per cm^2; Inner Shelf, GBR: 0.1±0.3 CAMAs per cm^2, Lizard Island, GBR: 0 CAMAs per cm^2; Orpheus Island, GBR 0.2±0.7 CAMAs per cm^2).

Distribution of CAMAs within anatomical regions of the coral polyp

Specific detection of bacteria by fluorescent *in situ* hybridization (FISH) can be problematic for coral samples due to nonspecific binding of probes and background

136 autoflorescence of granular cells and nematocysts [37]. Therefore, CAMAs were
137 identified by their characteristic shapes, in addition to fluorescent signals derived from
138 binding to the general bacteria-targeted probe set EUB338mix and comparisons to
139 background autofluorescence and non-specific binding (using Non338 probe). A total of
140 307 CAMAs were identified and localized by FISH (170 in Sesoko Island samples, 126
141 in samples from Inner Shelf sites in the Northern GBR, 4 from Lizard Island, 2 from
142 Outer Shelf sites in the Northern GBR, and 5 from Orpheus Island samples). CAMAs
143 were found within six anatomical regions of the coral polyp: the tentacle,
144 actinopharynx, mesentery, mesenterial filament, coenosarc and calicoblastic layer (see
145 **Fig. 3a**). Thirty-one additional CAMA-like shaped structures were observed (from three
146 samples derived from Sesoko Island), but these were discounted as bacterial aggregates
147 due to non-probe binding signals and excluded from further downstream analysis. The
148 CAMAs appeared to be randomly distributed across the anatomical regions
149 investigated, although because the numbers of CAMAs characterized for the Lizard
150 Island, Outer Shelf and Orpheus Island samples were low (**Fig. 3b**), meaningful
151 comparisons can only be made between the Sesoko Island and Northern Inner Shelf
152 samples. For the Sesoko Island samples, CAMAs were found predominantly in the
153 tentacles (36.5%), mesenterial filaments (34.7%) and coenosarc (16.5%) regions; in
154 Inner Shelf samples from Northern GBR sites, CAMAs were mostly located in the
155 calicoblastic layer (46.8%), tentacles (17.5%) and coenosarc (16.7%) (**Fig. 3b**).
156 CAMAs spanned a wide size range, from 23 to 6,761 μm^2 across tissue
157 samples from all sites (**Fig. 3c**). In general, measurements underestimated the size of

158 CAMAs, given that measurements were dependent on the orientation of sectioning and
159 it is unlikely that most CAMAs were sectioned through their greatest diameter.
160 Acknowledging constraints associated with sectioning, the average size of CAMA's
161 was 1,304 μm^2. On average, Sesoko Island samples contained larger aggregates
162 (1,507.7±1,522.4 μm^2) than samples from the GBR region (Inner Shelf: 637.4±734
163 μm^2. However, given the large range in sizes measured, the fact that only two locations
164 had sufficient sample sizes for comparison, and the issue of sectioning orientation
165 potentially biasing size measurements, such patterns require further validation. No
166 patterns in the size of CAMAs across different anatomical regions were detected (**Fig.**
167 **3c**).
168
169 *Morphology of CAMAs within coral tissues*
170 High resolution imaging was used to partially characterize and compare the
171 morphology of bacteria across the CAMAs detected (**Fig. 4**). Interestingly, each CAMA
172 appeared to be composed of a single morphological type of bacteria, although
173 morphological types varied among CAMAs. Overall, five different morphological types
174 of bacteria were identified: rod-shaped (length 2.5±0.1 µm, width 0.6±0.0 µm, **Fig. 4a,**
175 **e**), an atypical cocci (length 4.8±0.3 µm, width 3.1±0.2 µm, **Fig. 4b, f**), a longer rod
176 morphology (length 8.0±0.0 µm, width 0.8±0.0 µm, **Fig. 4c, g**), filamentous-like
177 bacteria (length N.D., width 0.4±0.0 µm, **Fig. 4d, h**), and a rod-shaped morphology but
178 with spore-like structures (**Fig. 4i–j**, **m–n**). While the consistency of morphological
179 characteristics within each CAMA may indicate that CAMAs are hosting single

bacterial types, it is also possible that they host multiple bacterial species with similar morphologies. Interestingly, the fluorescent signal detected for some CAMAs was not uniform over the entire aggregation. The lack of signal within some CAMAs (see **Fig. 4d** for example) may be due to the probe not targeting microbial cells that inhabit that space. Defining a specific morphological shape for the bacterial cells observed was sometimes difficult, with patchy probe hybridization producing images of structures that potentially protruded from the tissue sections and seemed amorphous (**Fig. 4k–l, o–p**). However, this again could be the result of mixed microbial communities within the CAMA's, with some cells targeted by the probes, but others not hybridizing to the probe-fluorochrome conjugate.

Further three-dimensional reconstructions of z-stacked FISH images of select 100 µm stained sections of tentacles visualized the CAMAs as typically spheroid or ellipsoid-shaped structures (**Fig. 5a**). In one example, a single CAMA was located independently in the ectoderm of a tentacle (**Fig. 5b**). In a different tentacle, multiple smaller CAMAs were localized close to *Symbiodiniaceae* cells in the gastrodermal region (**Fig. 5c**). Sizes of the large single CAMA and the multiple smaller CAMAs were 33,400 μm^3 (**Fig. 5d**, surface area 7,729 μm^2) and 1,978 ± 141.2 μm^3 (**Fig. 5e**, 809.5 ± 59.9 μm^2, n=4 CAMAs), respectively. Even though the CAMAs were located in the same polyp, the size of the single large CAMA was approximately 40-fold greater than the multiple smaller CAMAs, demonstrating inherent size variability for these structures. The bacteria within these CAMAs displayed a similar rod-shaped morphology (see **Fig. 4a and e**), with the average cross-sectional area of each bacterium

202 being 175.7 μm^2 and 22.6±4.2 μm^2, respectively (**Suppl. Fig. 2**). Based on cell size, the
203 number of individual rod-shaped bacterial cells within the 3D rendered images of these
204 CAMAs was estimated as ~ 47,275 cells for the large single CAMA located in the
205 ectoderm of the tentacle (**Fig. 5d** and **Suppl. Fig. 2a**), and 2,799±200 cells (**Fig. 5e** and
206 **Suppl. Fig. 2b**) for each of the smaller CAMAs localized close to *Symbiodiniaceae*
207 cells.
208

209 ## Discussion

210 The importance of microbial symbionts to their hosts has been demonstrated
211 for many animals, through acquisition and passage of nutrients, niche space occupation
212 and shared metabolic pathways [38–40]. For corals, the fundamental roles that
213 endosymbiotic dinoflagellates (*Symbiodiniumecae*) play in fitness of the coral holobiont
214 have long been established [e.g., 41,42], but although many studies have postulated the
215 importance of bacterial communities to coral fitness (see in the review) [3], direct
216 evidence is still mostly lacking [15]. To facilitate a more comprehensive understanding of
217 the roles bacterial communities may play in the coral holobiont, an improved
218 understanding of the localization of these microbial communities is essential,
219 particularly tissue-associated bacterial communities housed within structures termed
220 coral-associated microbial aggregates (CAMAs). In this study, we provide high
221 resolution characterization of these aggregations in tissues of *A. hyacinthus* sampled
222 from sites in Japan and the Great Barrier Reef, Australia, including estimates of CAMA

distributions, density and size, as well as visualization of the morphologies of bacterial cells within these structures.

We found that CAMAs commonly occur in healthy tissues of the coral *Acropora hyacinthus* collected from sites in Japan and Australia separated by more than 40 degrees of latitude. Although CAMAs were not detected in all tissue samples collected, this may reflect limitations in the area of coral tissue that can be surveyed via histological approaches. The presence of CAMAs in a histological section will depend on the tissue sectioned (i.e. the location of the fragment on the colony and on the section from the fragment), and on the scale and orientation of the section. Therefore, although not all coral tissue samples (and therefore not all colonies) were found to host CAMAs, we cannot exclude the possibility that other tissue areas of the same colony had CAMAs present. Other studies have also reported that CAMAs are common in tissues of many coral species in the Caribbean [32,33], Indo-Pacific and Red Sea [31,34,35]. In particular, CAMAs were common in species of *Acropora*, *Porites*, and *Pocillopora*, although often their presence was patchy within a population sample [31].

Interestingly, CAMAs were detected in a higher proportion of samples from inshore sites (i.e., 100% of Sesoko Island samples, 80% of samples from the northern GBR Inner Shelf site) than from offshore sites (25-40% of samples). Tissue density of CAMAs was also greatest in inshore samples (20.1±17.1 and 5.4±8.7 CAMAs per cm^2 for Sesoko Island and Inner Shelf GBR samples, respectively), and densities progressively decreased in tissues from the three more offshore sites (<1.2 CAMAs per cm^2), culminating in 0 CAMAs per cm^2 in the northern GBR Outer Shelf samples.

Although our study provides only a snapshot of five sites sampled at one time point, it suggests that inshore reef environments may promote the development of CAMAs within coral tissues. The inshore site at Sesoko Island has high nutrient influxes, especially phosphates [43,44]. Similarly, nearshore GBR sites are influenced by influxes of dissolved nutrients from terrestrial runoff, with higher concentrations typically found at inshore compared with offshore sites [45]. Temperature fluctuations may also influence CAMA abundance, although differences in seasonal temperature fluctuations are minimal across the northern GBR sites [46]. The coral microbiome community has been shown to shift in response to environmental stressors [29,47–52], thus water quality parameters influencing microbiological composition and function [53] could stimulate CAMA abundance. Further studies, particularly of potential links between nutrient levels and CAMA development, are needed to understand what might drive the increased prevalence and density of CAMAs in coral tissues at inshore sites, and to determine if hosting more CAMAs is beneficial to corals or is an indicator of negative impacts on the coral holobiont.

Localization of CAMAs using FISH demonstrated that they occur in all six of the anatomical regions investigated, i.e., the tentacle, actinopharynx, mesentery, mesenterial filament, coenosarc and the calicoblastic layer. CAMAs were highly variable in size, spanning a range from 23 to 6,761 μm^2 in area, with no obvious pattern in size when analyzed by anatomical region or geographic site. Although Sesoko Island samples contained larger aggregates on average (average cross-sectional area of 1,507.7±1,522.4 μm^2) than other sampling sites, low numbers of CAMAs in tissues

267 from some sites, combined with potential bias introduced by sectioning, limit the
268 conclusions that can be drawn. Nevertheless, investigation of the potential influence of
269 water quality parameters on the size of CAMAs is warranted.

270 Estimating the number of cells within CAMAs using 3D imaging revealed
271 that a CAMA with a cross-sectional area of 22.6±4.2 μm^2 would be composed of
272 ~2,800 rod-shaped bacteria. Based on similar methods, we further extrapolated that
273 bacterial densities in tissues from Sesoko Island and Inner Shelf GBR corals are
274 approximately 5.6 x 10^4 and 1.5 x 10^4 cells per cm^2 (along a linear cross-section),
275 respectively. Very few studies have accurately determined bacterial cell densities
276 associated with corals. Counts for bacteria in the coral mucus layer can be as high as 10^7
277 cells ml^{-1} [54]. Estimates of bacteria on tissue surfaces range from 1 x 10^5 to 10^6 cells per
278 cm^2 for the coral *Pocillopora damicornis* [55] and 8.3 x 10^6 to 6.2 x 10^7 cells per cm^2 for
279 the coral *Oculina patagonica* [24]. However, these counts are based on bacteria external to
280 coral tissues and therefore not directly comparable to estimates from our 3D
281 reconstructions of CAMAs visualized within coral tissues. Our results highlight that
282 tissue-associated communities exist and that differentiating these communities from
283 external and mucus-associated microbial communities is important for accurate
284 appraisals of the coral microbiome and for identifying their role(s) within the coral
285 holobiont.

286 An important finding from our high-resolution FISH imaging study is that in
287 most cases, each CAMA contained bacterial cells that were consistent in their
288 morphological appearance. Moreover, bacterial morphologies varied among CAMAs,

289 with up to five different cell morphologies detected. This variation in bacterial cell
290 morphology among CAMAs may explain why the histological staining properties of
291 CAMAs varied, the majority being basophilic (95.9%), but 4.1% staining eosinophilic
292 (n=318 CAMAs detected in total). Similar variability in the staining of CAMAs has
293 been reported previously [31,56], and has been attributed to varying degrees of protein and
294 DNA production or local tissue pH conditions [31]. However, our finding that different
295 morphological variants of bacteria are housed within different CAMA's potentially
296 contributes to variation in the H&E staining observed. Previous studies have reported
297 that the abundant coral-associated bacterial genera *Endozoicomonas* forms aggregates
298 within tissues of the corals *Stylophora pistillata* and *Pocillopora verrucosa* [35,57]. Indeed,
299 extensive sequence-based phylogenetic surveys of coral microbiomes have revealed that
300 several dominant bacterial groups are common [20], including the *Proteobacteria*
301 (particularly *Alpha*- and *Gamma-proteobacteria* inclusive of *Endozoicomonas*), as well
302 as *Actinobacteria*, *Bacteroidetes* (especially *Flavobacteria*), and *Cyanobacteria* [3].
303 Hence some of the different cellular morphologies we detected within CAMAs may
304 represent common coral-associated bacterial groups profiled in microbiome diversity
305 studies. In addition, two dominant bacteria were found to be localized intercellularly
306 within *Symbiodiniaceae* residing in the gastrodermal layers of coral host tissues using
307 both sequencing and FISH [27]. We note, however, that bacterial morphology can be
308 plastic and dependent on numerous variables, such as division stage, colonization,
309 chemical environment, physical constraints and nutrient availability [58]. Future work
310 targeting CAMAs with taxa-specific probes and gene sequencing approaches would

help to resolve both the taxonomy and potential functional roles of bacterial types within the holobiont.

FISH imaging showed that, for some of the CAMAs, patchy probe-specific labeling occurred, resulting in dull or dark areas within the structures. There are a number of potential methodological reasons for this observation, including: 1) insufficient probe sensitivity due to low ribosomal rRNA content in target cells [59,60], 2) methodological and environmental factors that prevent probes from accessing target cellular rRNA at these sites [61], 3) the bacterial community penetrating and proliferating within the outer epidermal layer of coral tissues [34], or 4) lipid or fat solvents deposited through dehydration and dewaxing steps showing empty spaces in the tissues [62]. Alternatively, little to no signal in central regions of some of the CAMAs could indicate that the probe EUB338mix did not target the taxonomic group of microbes within these regions. The EUB338mix is estimated to cover 96% of the *Eubacteria* domain, but taxa outside this coverage, including archaeal lineages, may be present [63]. We speculate that some of the CAMAs may be mixed communities containing bacteria not targeted by the probes or even *Archaea,* which have been identified to associate with corals in microbiome diversity studies [64]. A recent coral metagenomic study recovered *Thermarchaeota* genome bins from a *Porites sp* that was potentially metabolically linked through nitrogen cycling to other coral microbial-associated taxa, including *Nitrospira* [5]. Co-aggregation of ammonia-oxidizing archaea with nitrite-oxidizing bacteria is common in other organisms, such as sponges [65,66]. Findings that CAMAs are often co-localized near *Symbiodiniaceae* cells highlights the need for further isotope

333 studies to visualize and validate potential metabolic integrated links between bacterial,
334 archaeal and *Symbiodiniaceae* symbionts.
335

336 ## Conclusion

337 Localization of microorganisms associated with corals is vital to understand
338 their symbiotic relationships and reveal their function(s) within the holobiont. Here we
339 provide novel insight into the distributions and densities of bacteria within tissues of the
340 coral *Acropora hyacinthus* sampled from five different locations. CAMAs were
341 common in coral tissues sampled, although their abundance differed across geographic
342 sites. While each CAMA appeared to be dominated by a single bacterial morphological
343 type, different CAMA hosted different bacterial morphotypes. CAMAs have been
344 defined as facultative symbionts, not necessary for host fitness [31], however their high
345 prevalence and abundance in coral tissues may indicate they are integrated into shared
346 metabolic pathways and central to maintaining coral fitness through provisioning
347 benefits. Such propositions require testing by tracing metabolic pathways, as well as
348 improved taxonomic and functional assessment of the microorganisms housed within
349 these CAMAs.
350

351 ## Materials and methods (less than 1500 words)

352 Fragments (~ 3 cm x 3 cm; n=48 colonies) of the tabulate coral *Acropora*
353 *hyacinthus* (Dana, 1846) were collected from five geographic locations across two
354 countries (Australia and Japan). Samples from Japan (n=10) were collected from

355 Sesoko Island (26˚37'40.3"N, 127˚51'36.4"E, depth 1.5–3.0 m, colony size 62.8±41.7
356 cm) in Okinawa, Japan in July 2015. On the Great Barrier Reef (GBR) Australia,
357 samples were collected from the Northern sector along an inshore to offshore gradient
358 inclusive of Lizard Island (see Fig. 1; n=10 from an Inner Shelf site (14˚47'29.4"S,
359 145˚20'18.8"E, depth 3–5 m, colony size 77.69±43.0 cm), n=10 from Lizard Island
360 (14˚68'60.40"S, 145˚44'49.56"E, depth 2–4 m, colony size 61.67±17.5 cm) and n=8
361 from an Outer Shelf site (14˚38'30.0"S, 145˚38'22.5"E, depth 2–5 m, 41±20.5 cm)) in
362 February 2012. Samples (n =10) were also collected from reefs around Orpheus Island
363 (18˚35'55.4"S, 146˚29'33.8"E, depth 2–3 m, colony size N.D.) in the inner central
364 region of the Great Barrier Reef in March 2012.

365 Following collection, samples were immediately rinsed with sterile seawater
366 and then fixed in 4% paraformaldehyde (Electron Microscopy, USA and Wako, Japan)
367 in 10mM phosphate buffered saline (PBS; pH 7.4) for 8–10 hours maintained at 4 ˚C.
368 Samples were subsequently rinsed twice with 70% ethanol and stored in 70% ethanol at
369 4 ˚C prior to decalcification. After samples were rinsed by PBS twice for 30 min each,
370 samples were decalcified at 4 ˚C in a 10% EDTA (sigma-Aldrich, USA) solution (w/v;
371 pH 8.0 adjusted by sodium hydroxide [Wako, Japan]), which was exchanged
372 approximately every two days until no coral skeleton remained. The decalcified samples
373 were rinsed in PBS, and dehydrated sequentially through 70%, 90%, abs. 100% and abs.
374 100% ethanol series (60 min each), then processed through a 1:1 solution of abs. 100%
375 ethanol and toluene and two toluene (30 min each), and embedded in paraffin. Nine
376 sections (three serial sections x three sets; interval = 100 µm between each set) of each

377 coral fragment, each 4 µm thick, were cut from each paraffin-embedded sample (Suppl.
378 Fig. 3). In addition, thicker 100 µm sections were cut from coral tissues to allow
379 reconstructions of three-dimensional configurations of the CAMAs (see below). Serial
380 sections were mounted on one slide coated with egg-white glycerin and on two slides
381 with poly-L-lysine solution (Sigma-Aldrich, USA) for HE staining and fluorescence *in*
382 *situ* hybridization (FISH), respectively. We analyzed a total 144 sets (432 sections) of
383 the serial sections for H&E staining and FISH among five location sites.

384 For HE staining, one serial section from each set was dewaxed in xylene (2 x
385 15 min), rehydrated through ethanol series with abs. 100%, 99%, 90% and 70% (5 min
386 each) and rehydrated completely in sterile water. Hydrated sections were stained in
387 Mayer's hematoxylin (Wako, Japan) for 10 min, rinsed in water for 5 min, then stained
388 with eosin Y (Merck, Germany) for 5 min, and further rinsed in water for 30 sec. The
389 stained sections were dehydrated through the same ethanol series in reverse with
390 agitation (few sec each), cleared by xylene (2 x 5 min) and finally mounted in Entellan
391 mounting medium (Merck, Germany). HE stained sections were observed and recorded
392 using an ECLIPSE Ni microscope (Nikon, Japan) and BIOREVO BZ–9000 microscope
393 (KEYENCE, Japan).

394 The other two serial sections from each set were subjected to FISH according
395 to the protocol detailed in Wada et al. (2016) [37]. Briefly, sections were dewaxed in
396 xylene (2 x 15 min), dehydrated briefly once in 100% ethanol and dried completely.
397 The dried sections were immersed in a 0.2 M HCl solution for 12 min, followed by a 20
398 mM Tris-HCl solution (pH 8.0) for 10 min at room temperature. The sections were

399 mounted with proteinase K (50 µg ml^{-1}) in 20 mM Tris-HCl solution at 37 ˚C for 5 min
400 for bacterial cell wall permeabilization, and washed in a 20 mM Tris-HCl solution at
401 room temperature for 10 min. Oligonucleotide probes, including a probe targeting the
402 16S rRNA gene (EUB338mix: 5'-GCWGCCWCCCGTAGGWGT-3') and a nonsense,
403 negative control probe (Non338: 5'- ACATCCTACGGGAGGC -3'), were labeled with
404 the Cy3 fluochrome (eurofins, USA) [67,68]. Tissue sections were covered with
405 hybridization buffer (30% v/v formamide, 0.9 M NaCl, 20 mM Tris-HCl [pH 8.0],
406 0.01% SDS), then each oligonucleotide probe was added to a final concentration of 25
407 ng $µl^{-1}$ to each serial section. The slides were incubated at 46 ˚C for 1.5 hour. After
408 incubation, sections were washed in 50 ml falcon tubes containing preheated wash
409 buffer (0.112 M NaCl, 20 mM Tris HCl [pH 8.0], 0.01% SDS, 5 mM EDTA [pH 8.0])
410 in a water bath at 48 ˚C for 10 min, then soaked immediately with agitation in cold
411 water, and air dried completely. The dried sections were mounted in an antifade
412 mounting medium Fluoromount/Plus (Diagnostic BioSystems, USA). Sections were
413 examined and recorded using a FV1000-D confocal microscope (Olympus, Japan) with
414 two channels, using the following settings: (1) laser: 405 nm and 559 nm; (2) excitation
415 dichroic mirror: DM405/473/559; (3) emission dichroic mirror: SDM560 and mirror;
416 (4) band-pass filter: None and BA575–620 for detecting autofluorescence of coral tissue
417 (blue) and Cy3 signal (red), respectively. Non-specific probe binding in tissue sections
418 was identified as detailed by Wada et al. (2016)[37].

419 Three-dimensional images (3D) of CAMAs were reconstructed from the thick
420 sections (100 µm) which were cut carefully from two samples (S6 from the Sesoko

Island and LO8 from the Outer Shelf GBR site). Sections were visualized via FISH according to methods described above, and examined using a LSM 880 (ZIESS, Germany) with two tracks and the following settings: (1) laser: 405 nm and 561 nm; (2) beam splitter: MBS -405 and MBS 488/561; (3) filter: 371–479 nm for auto-fluorescence of coral tissue (blue) and 627–758 nm for *Symbiodiniaceae* (green) in track 1 and 565–588 nm for Cy3 signals (red) in track 2, respectively. For reconstructing the 3D images, the sections consisted of z-stack images at 3.0 µm intervals for 10x and 0.7 µm each and 40x magnifications using the Z-stack function in LSM 880. The z-stack images were processed and reconstructed with surface rending of the Cy3 signals in Imaris software ver. 8.0.2 (BitplaneAG, USA).

Statistical analysis was conducted using R Stats ver. 3.5.1 [69] with the following packages: DescTools ver. 0.99.26 [70], dplyr ver. 0.7.6 [71], FSA ver. 0.8.20 [72], lattice ver. 0.20–36 [73], and rcompanion ver. 2.0.0 [74]. To compare the abundances of CAMAs at the colony level among sites, G-tests followed by post hoc Bonferroni corrections were used. To evaluate the density of CAMAs within coral tissues, we compared the distribution of CAMAs among five sites using the Kruskal-Wallis test with Dunn's multiple comparison followed by a Benjamini-Hochberg correction method.

Author contribution

NW, NM and DB conceived the study. NW, JP and DB designed the sampling and FISH experiments. NW and JP conducted the field sampling. NW, MI and TM

443 performed the histological work and all observations and data collection. NW and DB
444 had major contribution in the manuscript writing and the figure making. JP, ST, TA,
445 BW and NM contributed to writing and editing the manuscript. All authors critically
446 reviewed, revised and ultimately approved this final version.
447

448 **Acknowledgements**

449 Dr. Joleah Lamb (Cornell University), Mr. Sefano Katz (Pacific Blue Foundation), Dr.
450 Gergely Torda (ARC Center of Excellence for Coral Reef Studies, James Cook
451 University), and Dr. Melanie Trapon (CSIRO) are thanked for helping to collect
452 samples. We are also grateful to Mr. Yasuhiko Sato from Ziess Microscopy Japan, and
453 Mr. Ji-Ying Huang and IPMB Live-Cell-Imaging Core Lab in the Institute Academia
454 Sinica for supporting the microscopy and Imaris software used, respectively.
455

456 **References**

457 1. Rohwer, F., Seguritan, V., Azam, F. & Knowlton, N. Diversity and distribution of
458 coral-associated bacteria. *Mar. Ecol. Prog. Ser.* **243**, 1–10 (2002).
459 2. Rosenberg, E., Koren, O., Reshef, L., Efrony, R. & Zilber-Rosenberg, I. The role of
460 microorganisms in coral health, disease and evolution. *Nat. Rev. Microbiol.* **5**, 355–
461 62 (2007).
462 3. Bourne, D. G., Morrow, K. M. & Webster, N. S. Insights into the Coral Microbiome:
463 Underpinning the Health and Resilience of Reef Ecosystems. *Annu. Rev. Microbiol.*
464 **70**, 317–340 (2016).
465 4. Yuyama, I., Ishikawa, M., Nozawa, M., Yoshida, M. & Ikeo, K. Transcriptomic
466 changes with increasing algal symbiont reveal the detailed process underlying
467 establishment of coral-algal symbiosis. *Sci. Rep.* **8**, 16802 (2018).

5. Robbins, S. J. *et al.* A genomic view of the coral holobiont. *Nat. Microbiol.* (in press).
6. Lema, K. A., Willis, B. L. & Bourne, D. G. Corals Form Characteristic Associations with Symbiotic Nitrogen-Fixing Bacteria. *Appl. Environ. Microbiol.* **78**, 3136–3144 (2012).
7. Pogoreutz, C. *et al.* Nitrogen Fixation Aligns with nifH Abundance and Expression in Two Coral Trophic Functional Groups. *Front. Microbiol.* **8**, (2017).
8. Yang, S.-H. *et al.* Metagenomic, phylogenetic, and functional characterization of predominant endolithic green sulfur bacteria in the coral Isopora palifera. *Microbiome* **7**, 3 (2019).
9. Raina, J.-B. *et al.* DMSP biosynthesis by an animal and its role in coral thermal stress response. *Nature* **502**, 677–680 (2013).
10. Raina, J.-B. *et al.* Isolation of an antimicrobial compound produced by bacteria associated with reef-building corals. *PeerJ* **4**, e2275 (2016).
11. Gochfeld, D. J. & Aeby, G. S. Antibacterial chemical defenses in Hawaiian corals provide possible protection from disease. *Mar. Ecol. Prog. Ser.* **362**, 119–128 (2008).
12. Ritchie, K. B. Regulation of microbial populations by coral surface mucus and mucus-associated bacteria. *Mar. Ecol. Prog. Ser.* **322**, 1–14 (2006).
13. Shnit-Orland, M. & Kushmaro, A. Coral mucus-associated bacteria: a possible first line of defense. *FEMS Microbiol. Ecol.* **67**, 371–380 (2009).
14. Galloway, S. B. *et al. Coral Disease and Health Workshop: Coral Histopathology II*. (NOAA Technical Memorandum NOS NCCOS 56 and NOAA Technical Memorandum CRCP 4, National Oceanic and Atmospheric Administration, Silver spring, 2007).
15. Peixoto, R. S., Rosado, P. M., Leite, D. C. de A., Rosado, A. S. & Bourne, D. G. Beneficial Microorganisms for Corals (BMC): Proposed Mechanisms for Coral Health and Resilience. *Front. Microbiol.* **8**, (2017).
16. Yang, S.-H. *et al.* Long-Term Survey Is Necessary to Reveal Various Shifts of Microbial Composition in Corals. *Front. Microbiol.* **8**, (2017).
17. Prazeres, M., Ainsworth, T., Roberts, T. E., Pandolfi, J. M. & Leggat, W. Symbiosis and microbiome flexibility in calcifying benthic foraminifera of the Great Barrier Reef. *Microbiome* **5**, 38 (2017).

18. Shiu, J.-H. *et al.* A Newly Designed Primer Revealed High Phylogenetic Diversity of Endozoicomonas in Coral Reefs. *Microbes Environ.* **33**, 172–185 (2018).

19. Hernandez-Agreda, A., Leggat, W., Bongaerts, P., Herrera, C. & Ainsworth, T. D. Rethinking the Coral Microbiome: Simplicity Exists within a Diverse Microbial Biosphere. *mBio* **9**, e00812-18 (2018).

20. Pollock, F. J. *et al.* Coral-associated bacteria demonstrate phylosymbiosis and cophylogeny. *Nat. Commun.* **9**, 4921 (2018).

21. Knowlton, N. & Rohwer, F. Multispecies Microbial Mutualisms on Coral Reefs: The Host as a Habitat. *Am. Nat.* **162**, S51–S62 (2003).

22. Ritchie, K. B. & Smith, G. W. Microbial Communities of Coral Surface Mucopolysaccharide Layers. in *Coral Health and Disease* (eds. Rosenberg, P. E. & Loya, P. Y.) 259–264 (Springer Berlin Heidelberg, 2004).

23. Bourne, D. G. & Munn, C. B. Diversity of bacteria associated with the coral Pocillopora damicornis from the Great Barrier Reef. *Environ. Microbiol.* **7**, 1162–1174 (2005).

24. Koren, O. & Rosenberg, E. Bacteria Associated with Mucus and Tissues of the Coral Oculina patagonica in Summer and Winter. *Appl. Environ. Microbiol.* **72**, 5254–5259 (2006).

25. Johnston, I. S. & Rohwer, F. Microbial landscapes on the outer tissue surfaces of the reef-building coral Porites compressa. *Coral Reefs* **26**, 375–383 (2007).

26. Chiu, H.-H., Mette, A., Shiu, J.-H. & Tang, S.-L. Bacterial Distribution in the Epidermis and Mucus of the Coral Euphyllia glabrescens by CARD-FISH. *Zool. Stud.* 11 (2012).

27. Ainsworth, T. D. *et al.* The coral core microbiome identifies rare bacterial taxa as ubiquitous endosymbionts. *ISME J.* **9**, 2261–2274 (2015).

28. Yang, S.-H. *et al.* Prevalence of potential nitrogen-fixing, green sulfur bacteria in the skeleton of reef-building coral Isopora palifera. *Limnol. Oceanogr.* **61**, 1078–1086 (2016).

29. Glasl, B., Herndl, G. J. & Frade, P. R. The microbiome of coral surface mucus has a key role in mediating holobiont health and survival upon disturbance. *ISME J.* **10**, 2280–2292 (2016).

30. Ainsworth, T. D., Fine, M., Roff, G. & Hoegh-Guldberg, O. Bacteria are not the primary cause of bleaching in the Mediterranean coral Oculina patagonica. *ISME J.* **2**, 67–73 (2007).

31. Work, T. & Aeby, G. Microbial aggregates within tissues infect a diversity of corals throughout the Indo-Pacific. *Mar. Ecol. Prog. Ser.* **500**, 1–9 (2014).

32. Peters, E., Oprandy, J. & Yevich, P. Possible causal agent of" white band disease" in Caribbean acroporid corals. *J. Invertebr. Pathol.* **396**, 394–396 (1983).

33. Peters, E. A survey of cellular reactions to environmental stress and disease in Caribbean scleractinian corals. *Helgol Meeresunters* **137**, 113–137 (1984).

34. Ainsworth, T. & Hoegh-Guldberg, O. Bacterial communities closely associated with coral tissues vary under experimental and natural reef conditions and thermal stress. *Aquat. Biol.* **4**, 289–296 (2009).

35. Neave, M. J. *et al.* Differential specificity between closely related corals and abundant Endozoicomonas endosymbionts across global scales. *ISME J.* (2016). doi:10.1038/ismej.2016.95

36. Work, T. M. & Aeby, G. S. Pathology of tissue loss (white syndrome) in Acropora sp. corals from the Central Pacific. *J. Invertebr. Pathol.* **107**, 127–31 (2011).

37. Wada, N. *et al. In situ* visualization of bacterial populations in coral tissues: pitfalls and solutions. *PeerJ* **4**, e2424 (2016).

38. Wilson, A. C. C. & Duncan, R. P. Signatures of host/symbiont genome coevolution in insect nutritional endosymbioses. *Proc. Natl. Acad. Sci.* **112**, 10255–10261 (2015).

39. Kohl, K. D. & Carey, H. V. A place for host–microbe symbiosis in the comparative physiologist's toolbox. *J. Exp. Biol.* **219**, 3496–3504 (2016).

40. Petersen, J. M. *et al.* Chemosynthetic symbionts of marine invertebrate animals are capable of nitrogen fixation. *Nat. Microbiol.* **2**, 16195 (2017).

41. Yellowlees, D., Rees, T. A. V. & Leggat, W. Metabolic interactions between algal symbionts and invertebrate hosts. *Plant Cell Environ.* **31**, 679–694 (2008).

42. Petrou, K., Nielsen, D. A. & Heraud, P. Single-Cell Biomolecular Analysis of Coral Algal Symbionts Reveals Opposing Metabolic Responses to Heat Stress and Expulsion. *Front. Mar. Sci.* **5**, (2018).

565 43. Tada, K., Sakai, K., Nakano, Y., Takemura, A. & Montani, S. Size-
566 fractionated phytoplankton biomass in coral reef waters off Sesoko Island, Okinawa,
567 Japan. *J. Plankton Res.* **25**, 991–997 (2003).
568 44. Tanaka, Y. Nutrient uptake by reef building corals and the ecophysiological
569 effects. *Oceanogr. Jpn.* 101-117 (in Japanese) (2012).
570 45. Brodie, J. E., Devlin, M., Haynes, D. & Waterhouse, J. Assessment of the
571 eutrophication status of the Great Barrier Reef lagoon (Australia). *Biogeochemistry*
572 **106**, 281–302 (2011).
573 46. Berkelmans, R., Weeks, S. J. & Steinberga, C. R. Upwelling linked to warm
574 summers and bleaching on the Great Barrier Reef. *Limnol. Oceanogr.* **55**, 2634–2644
575 (2010).
576 47. Bourne, D., Iida, Y., Uthicke, S. & Smith-Keune, C. Changes in coral-
577 associated microbial communities during a bleaching event. *ISME J.* **2**, 350–363
578 (2007).
579 48. Dinsdale, E. a *et al.* Microbial ecology of four coral atolls in the Northern
580 Line Islands. *PloS One* **3**, e1584–e1584 (2008).
581 49. Vega Thurber, R. L. *et al.* Metagenomic analysis of stressed coral holobionts.
582 *Environ. Microbiol.* **11**, 2148–2163 (2009).
583 50. Littman, R., Willis, B. L. & Bourne, D. G. Metagenomic analysis of the coral
584 holobiont during a natural bleaching event on the Great Barrier Reef. *Environ.*
585 *Microbiol. Rep.* **3**, 651–660 (2011).
586 51. Kelly, L. W. *et al.* Local genomic adaptation of coral reef-associated
587 microbiomes to gradients of natural variability and anthropogenic stressors. *Proc.*
588 *Natl. Acad. Sci.* **111**, 10227–10232 (2014).
589 52. Shiu, J.-H. *et al.* Dynamics of coral-associated bacterial communities
590 acclimated to temperature stress based on recent thermal history. *Sci. Rep.* **7**, 14933
591 (2017).
592 53. Glasl, B., Webster, N. S. & Bourne, D. G. Microbial indicators as a diagnostic
593 tool for assessing water quality and climate stress in coral reef ecosystems. *Mar.*
594 *Biol.* **164**, 91 (2017).
595 54. Garren, M. & Azam, F. New Method for Counting Bacteria Associated with
596 Coral Mucus. *Appl. Environ. Microbiol.* **76**, 6128–6128 (2010).

597 55. Garren, M. & Azam, F. Corals shed bacteria as a potential mechanism of
598 resilience to organic matter enrichment. *ISME J.* **6**, 1159–1165 (2012).
599 56. Sudek, M., Work, T. M., Aeby, G. S. & Davy, S. K. Histological observations
600 in the Hawaiian reef coral, Porites compressa, affected by Porites bleaching with
601 tissue loss. *J. Invertebr. Pathol.* **111**, 121–125 (2012).
602 57. Bayer, T. *et al.* The Microbiome of the Red Sea Coral Stylophora pistillata Is
603 Dominated by Tissue-Associated Endozoicomonas Bacteria. *Appl. Environ.*
604 *Microbiol.* **79**, 4759–4762 (2013).
605 58. van Teeseling, M. C. F., de Pedro, M. A. & Cava, F. Determinants of
606 Bacterial Morphology: From Fundamentals to Possibilities for Antimicrobial
607 Targeting. *Front. Microbiol.* **8**, (2017).
608 59. Amann, R. I., Ludwig, W. & Schleifer, K. H. Phylogenetic identification and
609 in situ detection of individual microbial cells without cultivation. *Microbiol Mol Biol*
610 *Rev* **59**, 143–169 (1995).
611 60. Wagner, M., Horn, M. & Daims, H. Fluorescence in situ hybridisation for the
612 identification and characterisation of prokaryotes. *Curr. Opin. Microbiol.* **6**, 302–309
613 (2003).
614 61. Bouvier, T. & del Giorgio, P. A. Factors influencing the detection of bacterial
615 cells using fluorescence in situ hybridization (FISH): A quantitative review of
616 published reports. *FEMS Microbiol. Ecol.* **44**, 3–15 (2003).
617 62. Prophet, E. B. *Laboratory methods in histotechnology*. (Amer Registry of
618 Pathology, 1992).
619 63. Riou, V., Périot, M. & Biegala, I. C. Specificity Re-evaluation of
620 Oligonucleotide Probes for the Detection of Marine Picoplankton by Tyramide
621 Signal Amplification-Fluorescent In Situ Hybridization. *Front. Microbiol.* **8**, (2017).
622 64. Siboni, N., Ben-Dov, E., Sivan, A. & Kushmaro, A. Global distribution and
623 diversity of coral-associated Archaea and their possible role in the coral holobiont
624 nitrogen cycle. *Environ. Microbiol.* **10**, 2979–2990 (2008).
625 65. Arp, D. J. & Bottomley, P. J. Nitrifers: more than 100 years from isolation to
626 genome sequences. *Microbe-Am. Soc. Microbiol.* **1**, 229 (2006).
627 66. Feng, G., Sun, W., Zhang, F., Karthik, L. & Li, Z. Inhabitancy of active
628 Nitrosopumilus-like ammonia-oxidizing archaea and Nitrospira nitrite-oxidizing
629 bacteria in the sponge Theonella swinhoei. *Sci. Rep.* **6**, 24966 (2016).

630 67. Wallner, G., Amann, R. & Beisker, W. Optimizing fluorescent in situ
631 hybridization with rRNA-targeted oligonucleotide probes for flow cytometric
632 identification of microorganisms. *Cytometry* **14**, 136–43 (1993).
633 68. Daims, H., Brühl, A., Amann, R., Schleifer, K. H. & Wagner, M. The
634 domain-specific probe EUB338 is insufficient for the detection of all Bacteria:
635 development and evaluation of a more comprehensive probe set. *Syst. Appl.*
636 *Microbiol.* **22**, 434–44 (1999).
637 69. R Core Team. R: A Language and Environment for Statistical Computing.
638 *Vienna, Austria: R Foundations for Statistical Computing.* (2013).
639 70. Signorell, A. DescTools: Tools for descriptive statistics (R package version
640 0.99.26). *The Comprehensive R Archive Network* (2018).
641 71. Wickham, H., François, R., Henry, L., Müller, K. & RStudio. dplyr: a
642 grammar of data manipulation (R package version 0.7.6). *The Comprehensive R*
643 *Archive Network* (2018).
644 72. Ogle, D., Wheeler, P. & Dinno, A. FSA: Simple Fisheries Stock Assessment
645 Methods (R package version 0.8.20). *The Comprehensive R Archive Network* (2018).
646 73. Sarkar, D. *Lattice: multivariate data visualization with R*. (Springer Science
647 & Business Media, 2008).
648 74. Mangiafico, S. rcompanion: Functions to Support Extension Education
649 Program Evaluation (R package version 2.0.0). *The Comprehensive R Archive*
650 *Network* (2018).

651

652

653 **Figure legends**

654

655 **Fig. 1 Map showing the locations of five study sites in two countries**: **(a, b)** Sesoko

656 Island (SI) in Okinawa, Japan; **(a, c)** Inner Shelf (IS), Lizard Island (LI) and Outer Shelf

(OS) sites in the Northern Great Barrier Reef; and **(a, d)** Orpheus Island (OI) in the central Great Barrier Reef, Australia.

Fig. 2 Histological appearance, occurrence and density of CAMAs in the coral *Acropora hyacinthus.* (**a**) Numerous CAMAs (indicated by arrows) are visible in a histological section stained by hematoxylin and eosin of a colony from Sesoko, Japan. (**b**) Right panel shows close-up of a CAMA located in a mesentery of a polyp from the branch sectioned in (a). **(c)** Pie diagrams showing the proportion of colonies sampled that contained CAMAs at five sites in Japan and Australia. A significantly higher proportion of Sesoko Is. samples contained CAMAs than samples collected from three more offshore sites (Lizard Is., Outer Shelf northern GBR site, and Orpheus Is.) (**p<.005; G test followed by a post-hoc bonferroni). **(d)** Densities of basophilic-staining (upper graph) or eosinophilic-staining (lower graph) CAMAs at five sites. Densities of basophilic CAMAs were significantly greater in samples from Sesoko Is. than in samples from the three offshore sites (Lizard Is., Outer Shelf site, and Orpheus Is, as were densities in the Inner shelf GBR site compared to the two offshore northern sector sites (** p<005; Kruskal-Wallis test, with Dunn's multiple comparison followed by a bonferroni correction). Scale bars indicate 600 μm (**a**), 50 μm (**b**) and 10 μm **(d)**.

Fig. 3 Distribution of CAMAs within six anatomical regions of the coral *Acropora hyacinthus* collected from five sites in Japan and Australia. (a) Schematic drawing of a coral polyp showing the six anatomical regions examined microscopically (same

679 colour coding used in b) and c)). **b)** Pie charts showing the distribution of CAMAs
680 among six anatomical regions in samples from the five sites. **(c)** Dot plots comparing
681 the size of CAMAs among anatomical regions for each location. N=307 CAMAs
682 detected in tissues treated with FISH.
683
684 **Fig. 4 Morphological variation in bacteria housed within different CAMAs.** Note
685 that bacteria within each CAMA are morphologically similar. Dotted lines (in **a**–**d** and
686 **i**–**l**) delineate regions magnified in close-up images (**e**–**h** and **m**–**p**). Overall, five
687 bacterial morphologies were detected: rod-like (**a**, **e**), pleomorphic (**b**, **f**), long rods (**c**,
688 **g**), filamentous-like (**d**, **h**), rod-shaped with spore-like structures (**i**–**j** and **m**–**n**), and
689 putative amorphous masses (k–l and o–p). Scale bars indicate 10 µm (**a**–**d** and **i**–**l**) and 5
690 µm (**e**–**h** and **m**–**p**).
691
692 **Fig. 5 Three-dimensional (3D) images of CAMAs (red) within a tentacle of the**
693 **coral *Acropora hyacinthus,* as visualized using FISH.** (**a)** Section of tentacle showing
694 localization of two types of CAMAs (10x magnification). **(b)** Single aggregation of
695 bacteria in a large structure within the ectoderm (40x magnification; composed of 92 z-
696 stack images). **(c)** Multiple aggregations of bacteria in smaller structures within the
697 gastrodermis (40x magnification; composed of 56 z-stack images). 3D rendering of
698 CAMAs (**d** and **e**) reconstructed from 3D images in **b** and **c**. Coral tissue and
699 *Symbiodiniaceae* appear as blue and green structures, respectively.
700

Suppl. Fig. 1 Calculating the area of CAMAs. **(a)** A single large CAMA, comprised of rod-shaped bacteria, was calculated to be 175.7 μm^2 in cross-sectional area from 3D images. **(b)** Smaller, numerous aggregations were calculated to be, on average, 22.6±4.2 μm^2 in cross-sectional area (n = 8). Scale bars indicate 20 µm.

Suppl. Fig. 2 Schematic drawing showing how coral fragments were sectioned for H&E staining and FISH. In total, nine sections were collected from each sample (three sets of sections, each set comprised of three serial sections). *1: Distance between each set was 100 µm.

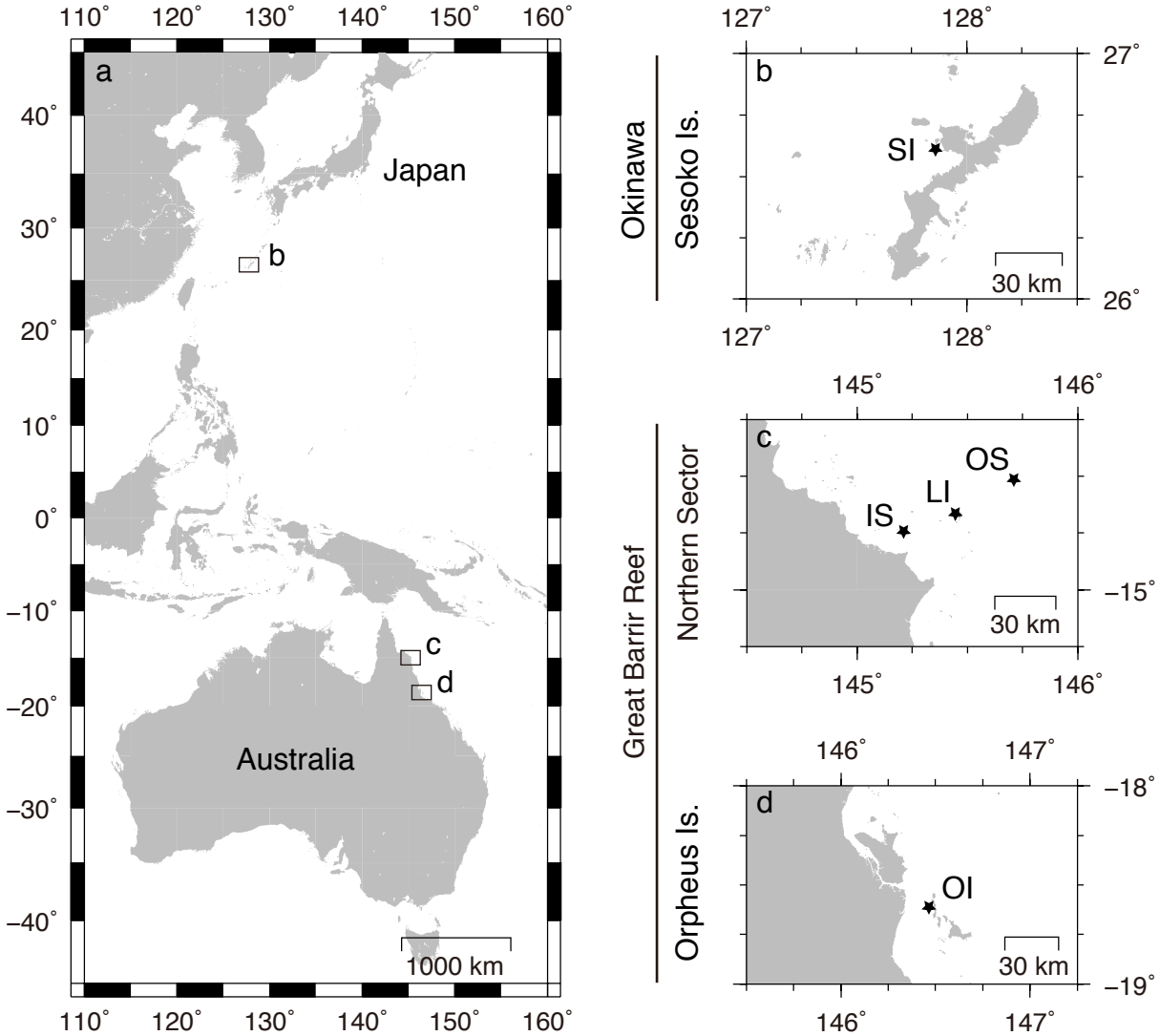
a
Japan
b
c
d
Australia
1000 km
110˚
120˚
130˚
140˚
150˚
160˚
40˚
30˚
20˚
10˚
0˚
−10˚
−20˚
−30˚
−40˚
Okinawa
Sesoko Is.
b
SI
30 km
127˚
128˚
27˚
26˚
Great Barrir Reef
Northern Sector
c
OS
LI
IS
30 km
145˚
146˚
−15˚
Orpheus Is.
d
OI
30 km
146˚
147˚
−18˚
−19˚

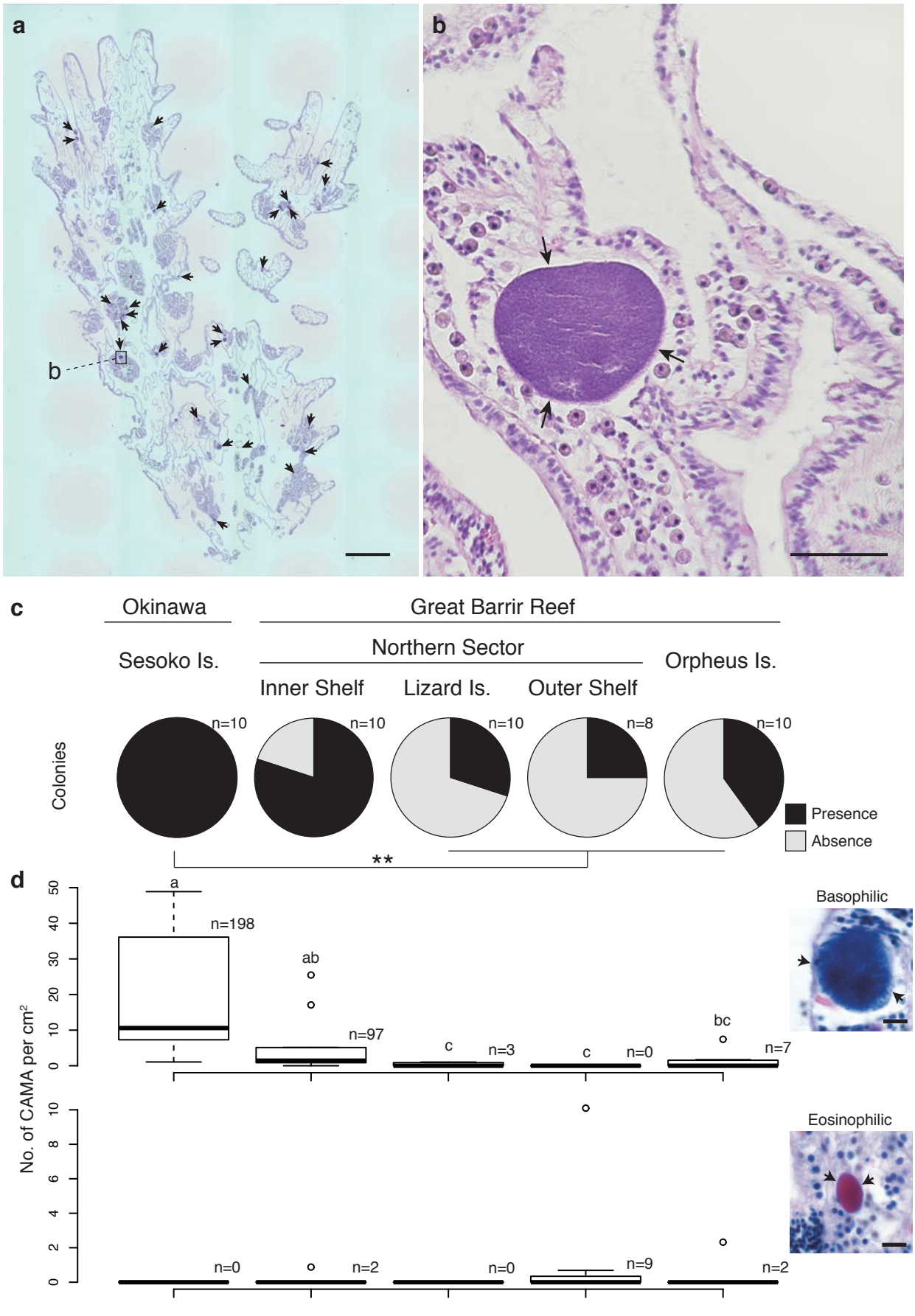
a
b
b
c
Okinawa
Great Barrir Reef
Sesoko Is.
Northern Sector
Orpheus Is.
Inner Shelf
Lizard Is.
Outer Shelf
Colonies
n=10
n=10
n=10
n=8
n=10
Presence
Absence
**
d
No. of CAMA per cm²
a
n=198
ab
n=97
c
n=3
c
n=0
bc
n=7
n=0
n=2
n=0
n=9
n=2
Basophilic
Eosinophilic

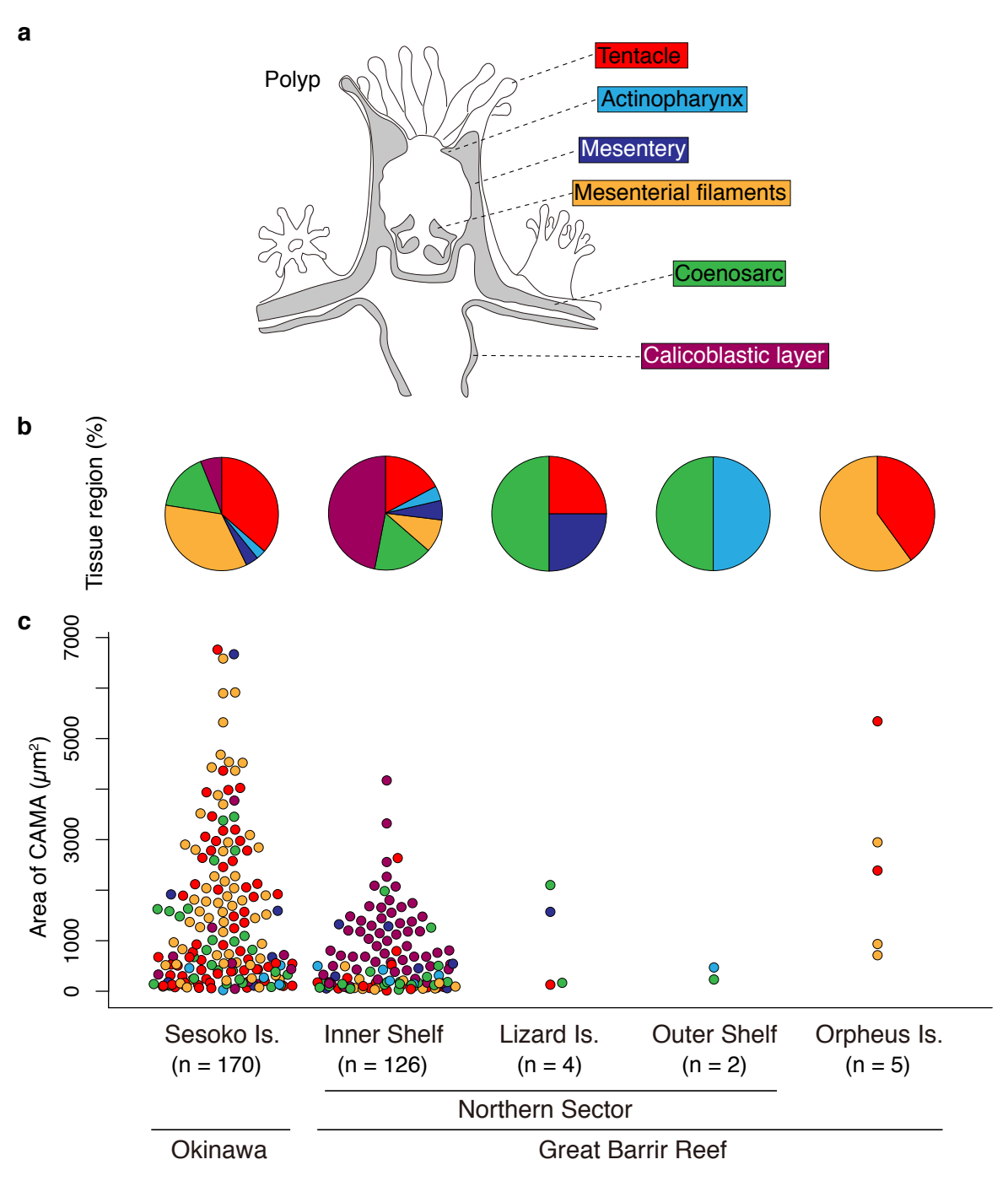
a
Polyp
Tentacle
Actinopharynx
Mesentery
Mesenterial filaments
Coenosarc
Calicoblastic layer
b
Tissue region (%)
c
Area of CAMA (μm²)
0
1000
3000
5000
7000
Sesoko Is.
(n = 170)
Inner Shelf
(n = 126)
Lizard Is.
(n = 4)
Outer Shelf
(n = 2)
Orpheus Is.
(n = 5)
Northern Sector
Okinawa
Great Barrir Reef

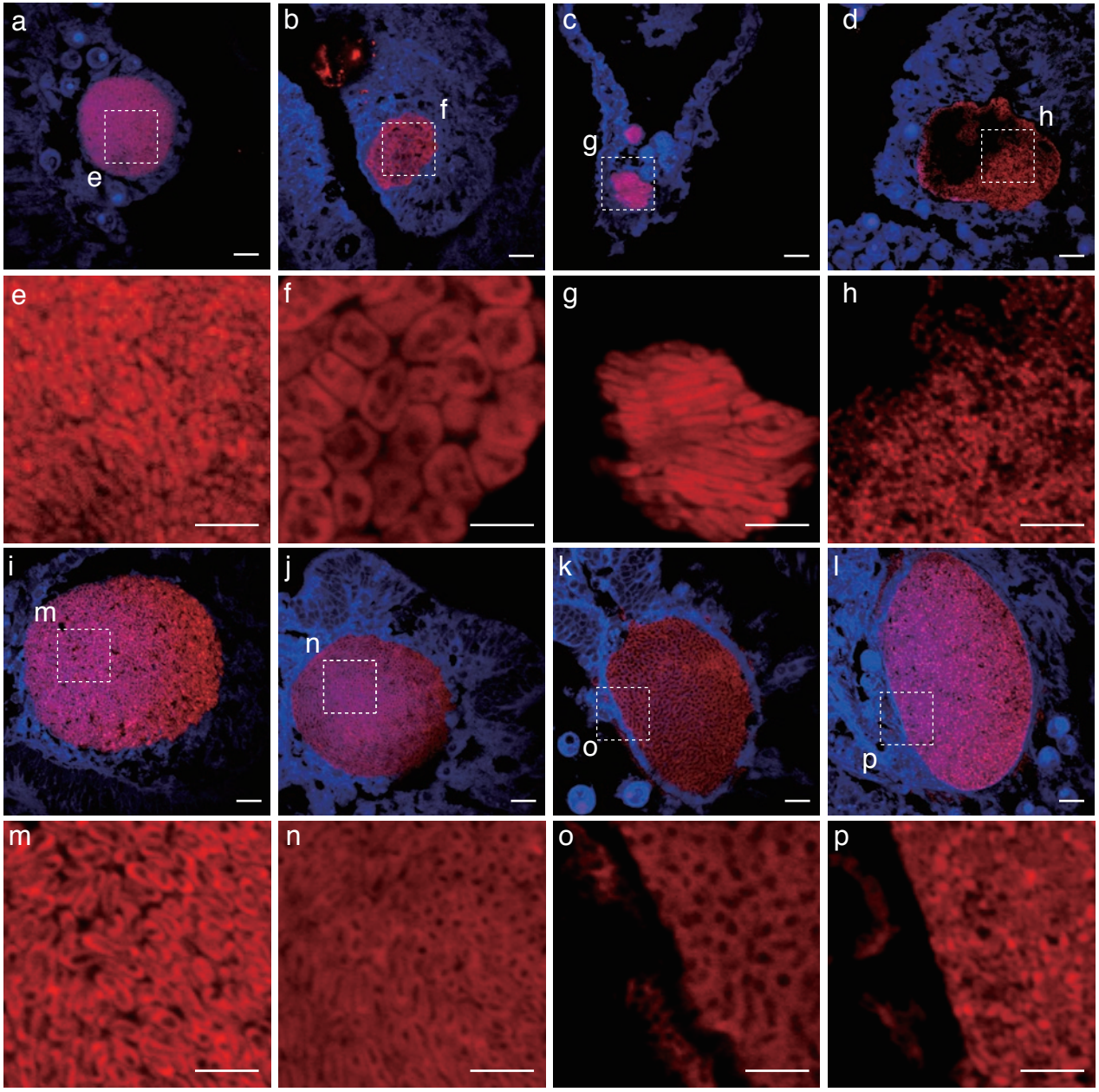
a
e
b
f
c
g
d
h
e
f
g
h
i
m
j
n
k
o
l
p
m
n
o
p

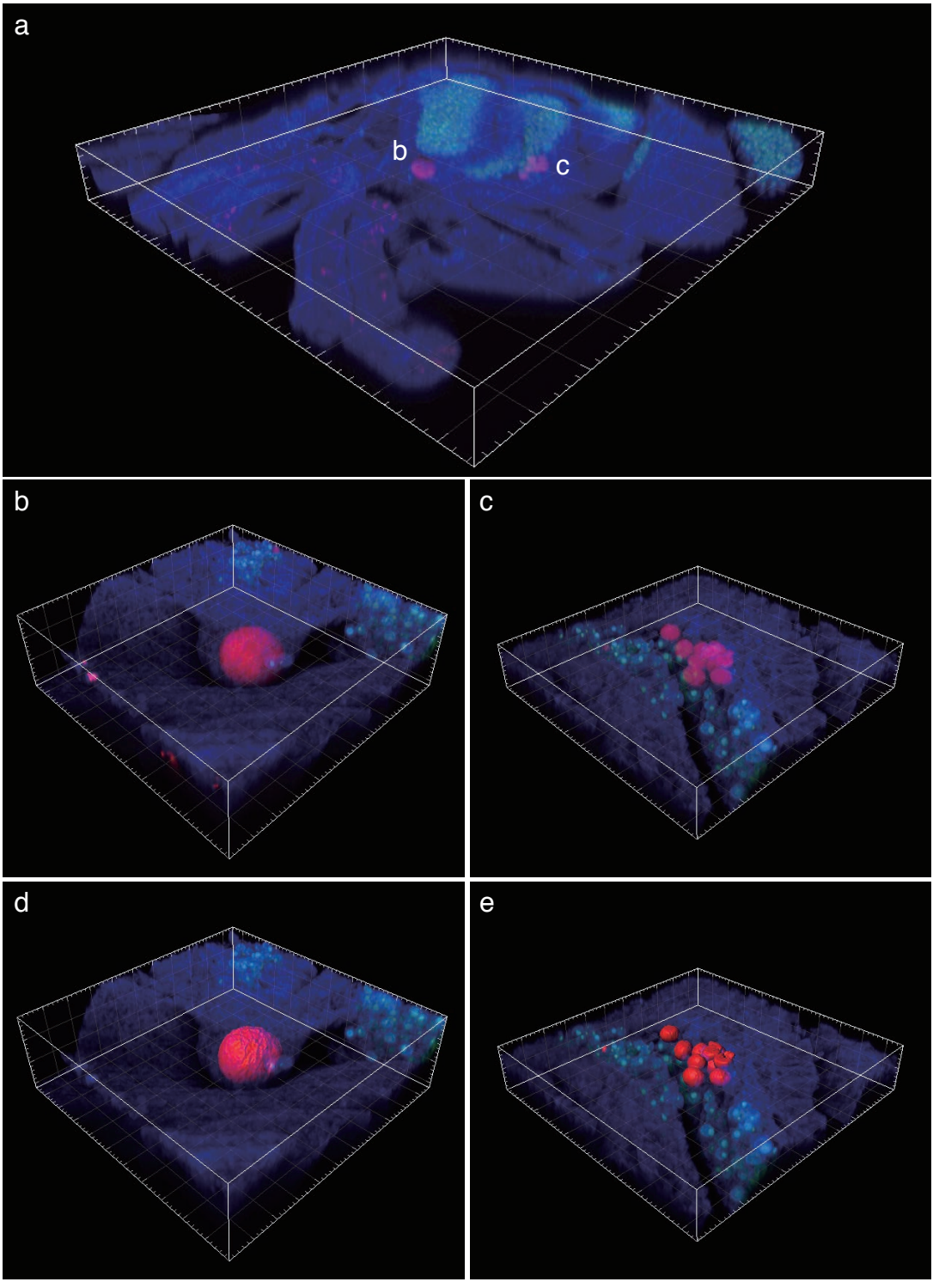
a
b
c
b
c
d
e